Journal of Crystal Growth 311 (2009) 2099–2101

Contents lists available at ScienceDirect

Journal of Crystal Growth

journal homepage: www.elsevier.com/locate/jcrysgro

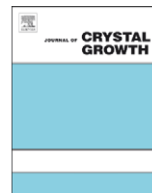

A comparison of ZnMgSSe and MgS wide bandgap semiconductors used as barriers: Growth, structure and luminescence properties

R.T. Moug [a], C. Bradford [a], F. Izdebski [a], I. Davidson [a], A. Curran [a], R.J. Warburton [a], K.A. Prior [a,*], A. Aouni [b], F.M. Morales [b], S.I. Molina [b]

[a] *David Brewster Building, School of Engineering and Physical Sciences, Heriot-Watt University, Edinburgh EH14 4AS, UK*
[b] *Departamento de Ciencia de los Materiales e Ingeniería Metalúrgica y Química Inorgánica, Universidad de Cádiz, E-11510 Puerto Real (Cádiz), Spain*

A R T I C L E I N F O

Available online 19 October 2008

PACS:
61.72.uj
64.75.Qr
64.75.St
68.37.Og
68.37.Ps
68.55.ag
68.55.Nq
78.55.Et
81.05.Dz
81.15.Hi

Keywords:
A1. Crystal morphology
A1. Low dimensional structures
A1. Phase equilibria
A3. Molecular Beam epitaxy
B2. Semiconducting II–VI materials
B2. Semiconducting quaternary alloys

A B S T R A C T

The wide bandgap alloy $Zn_{0.2}Mg_{0.8}S_{0.64}Se_{0.36}$ has recently been grown by molecular beam epitaxy (MBE) and been shown to be oxidation and acid resistant. This makes it attractive either as a replacement or adjunct to MgS in II–VI multilayers. In this paper we compare the structural and optical properties of MBE grown multilayer structures containing $Zn_{0.2}Mg_{0.8}S_{0.64}Se_{0.36}$ to those grown with the quaternary alloy replaced by MgS.

Cross-sectional high-resolution transmission electron microscopy (HRTEM) and X-ray interference spectra of ZnSe/$Zn_{0.2}Mg_{0.8}S_{0.64}Se_{0.36}$/ZnSe multilayers show the $Zn_{0.2}Mg_{0.8}S_{0.64}Se_{0.36}$ layers are of good crystal quality and do not phase segregate. Layer interfaces are seen to be flat and $Zn_{0.2}Mg_{0.8}S_{0.64}Se_{0.36}$ does not introduce defects into the overlying ZnSe. Atomic force microscopy shows the surface of a 30 nm $Zn_{0.2}Mg_{0.8}S_{0.64}Se_{0.36}$ layer is atomically flat, in contrast with similar MgS layers, which show pronounced 1D surface ridges, indicating that the $Zn_{0.2}Mg_{0.8}S_{0.64}Se_{0.36}$ layers have not started to relax.

ZnSe quantum wells grown with $Zn_{0.2}Mg_{0.8}S_{0.64}Se_{0.36}$ barriers show 77 K photoluminescence comparable in wavelength and intensity to ZnSe wells of similar thickness grown with MgS barriers. This has allowed us to demonstrate the use of the quaternary alloy, which resists oxidation in place of MgS in multilayer structures.

© 2008 Elsevier B.V. All rights reserved.

1. Introduction

The ability to separate an epitaxially deposited layer from the substrate on which it was grown and transfer it onto a different supporting material gives the potential for new device structures and is a necessary step for many applications. One simple method of accomplishing this is by means of an epitaxial lift-off technique, which was first demonstrated in GaAs/AlAs structures by Yablonovich et al. [1].

For II–VI semiconductors a similar lift-off technology has not been available in until recently, when we demonstrated that ZnSe/ZnCdSe quantum wells deposited on top of a MgS layer could be removed without damage from the GaAs substrate [2]. In these structures the MgS is used as a sacrificial layer due to its solubility in dilute HCl, there being a difference in etch rates between MgS and ZnSe of approximately 10^8:1.

Subsequently, we have aimed to develop a technology allowing II–VI multilayers containing either quantum wells or quantum dots to be removed from the substrate and transferred to materials of different functionality. Recently, we have used this technique to transfer ZnSe/ZnCdSe quantum wells onto Bragg dielectric mirror stacks, giving the potential of combining the benefits of commercially available dielectric mirrors with molecular beam epitaxy (MBE) grown active regions in hybrid devices which has enabled us to observe exciton–photon coupling in the quantum well [3,4].

In addition to its use as a sacrificial layer in these devices, MgS has other useful applications, as it can be grown epitaxially on GaAs in conjunction with ZnSe-based alloys. Also, having a bandgap of ~5 eV, it forms an excellent barrier material for both ZnSe quantum wells [5,6] and CdSe quantum wells and dots [7,8].

Unfortunately, it is of course not possible to use MgS both as a large bandgap barrier and as a sacrificial layer for epitaxial lift-off in the same structure. We have therefore examined other MgS-rich, ZnMgSSe alloys to determine suitable compositions which are acid resistant and were recently able to show that $Zn_{0.2}Mg_{0.8}S_{0.64}Se_{0.36}$ has many advantageous characteristics. In

*Corresponding author. Tel.: +44 131 451 3035; fax: +44 131 451 3473.
E-mail address: K.A.Prior@hw.ac.uk (K.A. Prior).

0022-0248/$ - see front matter © 2008 Elsevier B.V. All rights reserved.
doi:10.1016/j.jcrysgro.2008.10.040

addition to having a bandgap much larger than ZnSe, it has a smaller strain than MgS when grown epitaxially on GaAs and shows excellent resistance to acid attack [9].

Here, our aim is to compare the characteristics of $Zn_{0.2}Mg_{0.8}S_{0.64}Se_{0.36}$ layers with MgS layers grown under similar conditions. In particular, we show that substituting MgS with $Zn_{0.2}Mg_{0.8}S_{0.64}Se_{0.36}$ as a barrier material for ZnSe causes no significant changes in the properties of the quantum well. We also demonstrate that devices can be fabricated containing MgS sacrificial layers and $Zn_{0.2}Mg_{0.8}S_{0.64}Se_{0.36}$ barriers in the same structure, and that both layers function as expected.

2. Experimental procedure

Characterization of the samples described here was by atomic force microscopy (AFM), transmission electron microscopy (TEM), X-ray double crystal spectrometry and photoluminescence measurements. All sample growth and subsequent characterization was carried out at Heriot-Watt University, with the exception of TEM analysis, which was performed at University of Cadiz.

All samples were grown by MBE in a VG V80H system. The growth method used for the MgS-rich alloys was identical to that used for MgS [5] and the ZnMgSSe studies described previously [9]. Elemental sources of Zn, Mg and Se 6N pure were used, and S was provided from a ZnS 6N pure compound source. No other source of S was used in the growth chamber. Cell temperatures used were: Zn 285 °C, Se 177 °C, Mg 375 °C and ZnS 865 °C. The growth conditions for the quaternary alloy were chosen so that MgS and ZnMgSSe alloys could be integrated in the same structure, as is required for epitaxial lift-off [10].

At the start of growth, the GaAs substrate was heated to 580 °C to desorb the surface oxide, and then cooled to 240 °C under a Zn flux [11]. During growth, the substrate temperature was measured by a pyrometer and kept at 240 °C for all layers. All samples commenced with a 50 nm thick ZnSe buffer layer. The RHEED pattern became streaky before 2 nm of ZnSe had been deposited and remained streaky throughout the growth of all layers.

Three types of samples were grown. First, a set of GaAs/ZnSe (50 nm)/ZnMgSSe (*d* nm)/ZnSe (50 nm) samples were grown with *d* varied from 6 to 17 nm for analysis by X-ray interference (XRI) [12,13]. The thicknesses of the layers in these samples were such that they could be compared directly with an almost identical set of samples grown previously for analysis of ZnSe/MgS/ZnSe layers by XRI [6,14].

Subsequently, a sample was grown with a thicker ZnMgSSe layer with the structure GaAs/ZnSe (50 nm)/ZnMgSSe (31 nm)/ZnSe (4.5 nm) which was used for AFM and HRTEM analysis. Finally, for PL measurements the ZnMgSSe was used as a barrier material in the form of a GaAs/ZnSe (50 nm)/ZnMgSSe (31 nm)/ZnSe (4 nm)/ZnMgSSe (31 nm) structure.

AFM measurements of the samples were performed on a Dimensions 3100 system. To minimize the effects of surface contamination, all AFM measurements were obtained on samples immediately after removing them from the MBE system. X-ray spectra were recorded using Copper Kα radiation on a Bede 200 system. PL spectra were taken at 77 K using the 351 nm line from an Ar ion laser, and were collected by a 0.88 m Spex monochrometer.

A JEOL field-emission gun microscope operated at 200 keV (JEM-2010F) was used for high-resolution TEM analyses (HRTEM). Samples were prepared for cross-sectional TEM (XTEM) visualization in the same way as MgS/ZnSe multilayer samples examined previously [15], namely by mechanical grinding and dimpling down to 20 μm followed by ion beam thinning. In order to minimize further damage, the specimens were thinned with decreasing ion voltage from 4 to 2 KV and decreasing incidence angle from 12° to 6°. During preparation the sample holder was kept at 77 K.

Fig. 1 shows a typical XRI spectrum from a sample with a ZnMgSSe layer 10 nm thick. The XRI method is extremely sensitive to the thickness and interplanar spacing of the ZnMgSSe layer [13], and allows us to calculate the thickness and growth rate of the alloy layer. This method also allows us to accurately determine the composition using the Bede RADS simulation software to be $Zn_{0.2}Mg_{0.8}S_{0.64}Se_{0.36}$ [9], which was obtained within experimental error for all samples produced with these growth parameters.

The quality and number of the interference fringes observed in the XRI scan should also be noted. High quality fringes can only be observed when the two 50 nm thick ZnSe layers have nearly identical strains and parallel lattice planes, meaning the $Zn_{0.2}Mg_{0.8}S_{0.64}Se_{0.36}$ has not relaxed or undergone any phase segregation into regions of different composition and strain.

To confirm this, a GaAs/ZnSe (50 nm)/ZnMgSSe (31 nm)/ZnSe (4.5 nm) structure was grown and examined by TEM. Electron diffraction patterns from the whole heterostructure showed only one resolvable set of diffraction spots, indicative of an epitaxial, pseudomorphic structure with no evidence of any second crystalline phase or phase decomposition. Fig. 2 is a HR-XTEM micrograph of the ZnMgSSe/ZnSe boundary showing the atomic arrangement at this interface. There is not a great deal of contrast between the $Zn_{0.2}Mg_{0.8}S_{0.64}Se_{0.36}$ and the ZnSe at these high magnifications used, but a boundary can still be determined. There is complete continuity of the crystallographic planes of both structures and hence no evidence of misfit dislocations. In general, the boundary is sharp and flat, indicating a good quality interface with no significant intermixing, but in the example shown a triangular shape structural defect formed by two {111} approaching stacking faults which have propagated from the ZnMgSSe/ZnSe interface is visible in the bottom half of the figure. However, these defects are only occasionally observed and they are not intrinsic faults of the ZnMgSSe layer. Apart from the much poorer contrast between the layers, the interface appears similar to observed previously between ZnSe and MgS layers [14].

The alloy composition $Zn_{0.2}Mg_{0.8}S_{0.64}Se_{0.36}$ is predicted to lie within to the phase boundary for spontaneous (spinodal) decomposition into two phases [16], although we have previously shown that a reduction in the estimated value of the enthalpy of

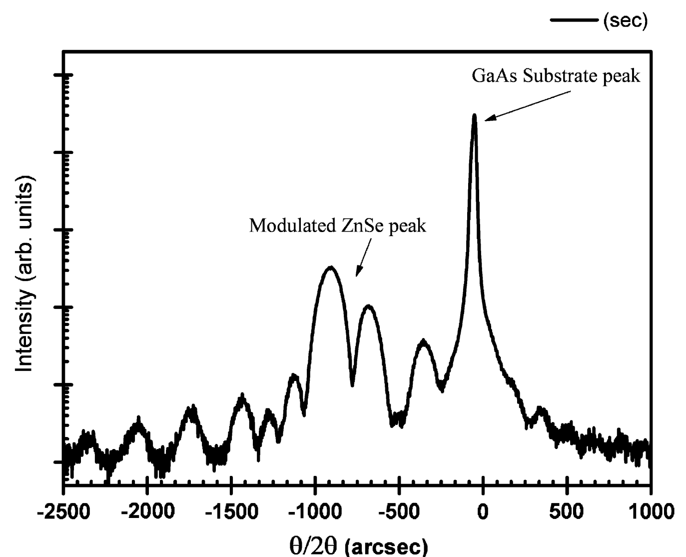

Fig. 1. XRI scan of a sample with the structure GaAs/ZnSe (50 nm)/$Zn_{0.2}Mg_{0.8}S_{0.64}Se_{0.36}$ (10 nm)/ZnSe (50 nm).

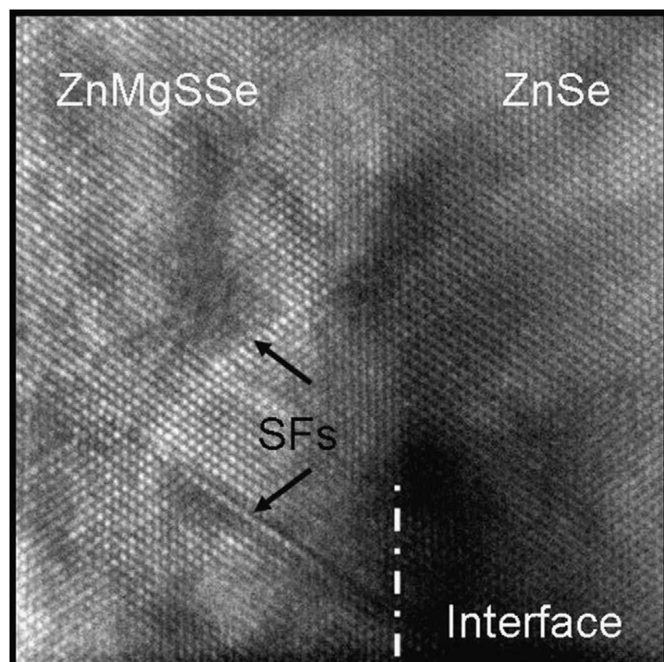

Fig. 2. HRTEM micrographs of the GaAs/ZnSe (50 nm)/ZnMgSSe (31 nm)/ZnSe (4.5 nm) sample showing the $Zn_{0.2}Mg_{0.8}S_{0.64}Se_{0.36}$/ZnSe interface where an abrupt boundaries between two layers with similar lattice parameter is visible.

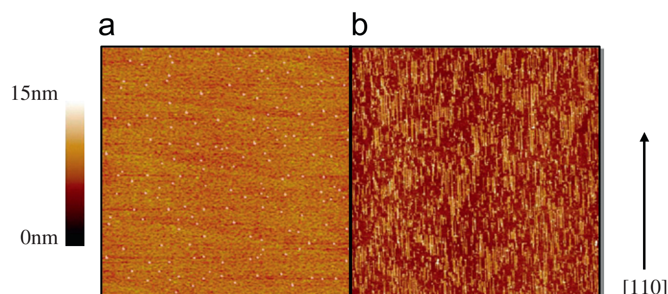

Fig. 3. 20 μm × 20 μm AFM scans of: (a) a GaAs/ZnSe (50 nm)/ZnMgSSe (31 nm)/ZnSe (4.5 nm) structure. The dot like features are selenium clusters and the surface in between has a roughness of 0.5 nm. (b) A GaAs/ZnSe (50 nm)/MgS (25 nm)/ZnSe (4 nm) layer, showing the pronounced 1D ridges.

formation of zinc blende MgS by only 2% will place this composition in the single phase region [9]. Furthermore the ZnMgSSe does not display any contrast modulation which is attributable to strain or composition fluctuations which would occur if phase decomposition had started. We are therefore confident that $Zn_{0.2}Mg_{0.8}S_{0.64}Se_{0.36}$ is single phase.

The surface morphology of the GaAs/ZnSe (50 nm)/$Zn_{0.2}Mg_{0.8}S_{0.64}Se_{0.36}$ (31 nm)/ZnSe (4.5 nm) structure was also examined by AFM (Fig. 3a). The surface of this sample shows many small features which are recognisable as Se clusters which form after exposure of the sample to air. Between the clusters, however, the sample is smooth, with a roughness of only 0.5 nm. It is of course possible that the ZnMgSSe layer has a larger roughness than this value and the surface might be smoothed by the presence of the ZnSe cap. However, Fig. 3b demonstrates the effect of replacing the ZnMgSSe by a layer of MgS layer of a similar thickness. Here, the MgS layer is seen to display pronounced 1D ridges, which are characteristic of MgS surfaces under a wide range of growth conditions [17], but have never been observed on $Zn_{0.2}Mg_{0.8}S_{0.64}Se_{0.36}$ surfaces at any thickness. We have previously suggested that the nanowires arise from a partial anisotropic relaxation occurring in thicker MgS layers [14,18] and their absence in the quaternary alloy is further evidence that these structures are pseudomorphic.

A total of 77 K PL obtained from the GaAs/ZnSe (50 nm)/ZnMgSSe (31 nm)/ZnSe (4 nm)/ZnMgSSe (31 nm) has been compared with PL from a similar sample with a 4 nm ZnSe well and MgS barriers. There is little change in spectral positions between the two wells, with strong excitonic emission observed in both cases. However, emission from the well with the MgS barriers shows a slightly larger FWHM (16 meV) than with the ZnMgSSe barriers (15.1 meV) with possibly some contribution from the interface roughness.

Based on these results, we conclude that when used with ZnSe quantum wells as a barrier material, $Zn_{0.2}Mg_{0.8}S_{0.64}Se_{0.36}$ is as good, if not slightly better than MgS. It is certainly resistant to oxidation, unlike MgS, and in conjunction with its previously demonstrated insolubility in dilute hydrochloric acid [9]; this has enabled us to develop an epitaxial lift-off technique for ZnSe-based alloys. We have recently demonstrated this by growing structures containing both an MgS sacrificial layer and $Zn_{0.2}Mg_{0.8}S_{0.64}Se_{0.36}$ barriers surrounding a ZnSe quantum wells [10]. In these structures, the integrity of the quantum well is not affected by the lift-off process, and the intensity of the well emission is unchanged after lift-off.

In summary, as a stage towards the development of a viable lift-off technology, we have demonstrated that $Zn_{0.2}Mg_{0.8}S_{0.64}Se_{0.36}$ can be used in combination with ZnSe in multilayer structures. The interfaces between the two materials are sharp and flat, and we observe no evidence of phase segregation in the quaternary alloy. A total of 77 K PL from ZnSe quantum wells with $Zn_{0.2}Mg_{0.8}S_{0.64}Se_{0.36}$ barriers is comparable in intensity to wells with MgS barriers, and multilayer structures using $Zn_{0.2}Mg_{0.8}S_{0.64}Se_{0.36}$ for carrier confinement and MgS for epitaxial lift-off have been demonstrated.

References

[1] E. Yablonovitch, T. Gmitter, J.P. Harbison, R. Bhat, Appl. Phys. Lett. 51 (1987) 2222.
[2] C. Bradford, A. Balocchi, A. Curran, R.J. Warburton, K.A. Prior, B.C. Cavenett, J. Crystal Growth 278 (2005) 325.
[3] A. Curran, J.K. Morrod, K.A. Prior, A.K. Kar, R.J. Warburton, Semicond. Sci. Technol. 22 (2007) 1189.
[4] A. Curran, R. Barbour, J.K. Morrod, K.A. Prior, A.K. Kar, R.J. Warburton, J. Korean Phys. Soc. 53 (2008) 3007.
[5] C. Bradford, C.B. O'Donnell, B. Urbaszek, A. Balocchi, C. Morhain, K.A. Prior, B.C. Cavenett, Appl. Phys. Lett. 76 (2000) 3929.
[6] C. Bradford, C.B. O'Donnell, B. Urbaszek, K.A. Prior, B.C. Cavenett, Phys. Rev. B 64 (2001) 195309.
[7] M. Funato, A. Balocchi, C. Bradford, K.A. Prior, B.C. Cavenett, Appl. Phys. Lett. 80 (2002) 443.
[8] M. Funato, K. Omae, Y. Kawakami, Sg. Fujita, C. Bradford, A. Balocchi, K.A. Prior, B.C. Cavenett, Phys. Rev. B 73 (2006) 245308.
[9] R.T. Moug, C. Bradford, D. Thuau, A. Curran, R.J. Warburton, K.A. Prior, J. Korean Phys. Soc. 53 (2008) 3004.
[10] R. Moug, C. Bradford, A. Curran, F. Izdebski, I. Davidson, K.A. Prior, R.J. Warburton, doi: 10.1016/j.mejo.2008.06.024.
[11] L.H. Kuo, K. Kimura, S. Miwa, T. Yasuda, T. Yao, Appl. Phys. Lett. 69 (1996) 1408.
[12] L. Tapfer, K. Ploog, Phys. Rev. B 40 (1989) 9802.
[13] B.K. Tanner, J. Phys. D: Appl. Phys. 26 (1993) A151.
[14] K.A. Prior, X. Tang, C. O'Donnell, C. Bradford, L. David, B.C. Cavenett, J. Crystal Growth 251 (2003) 565.
[15] A.M. Sanchez, J. Olvera, T. Ben, J.K. Morrod, K.A. Prior, S.I. Molina, Appl. Phys. Lett. 89 (2006) 121907.
[16] V.S. Sorokin, S.V. Sorokin, V.A. Kaygorodov, S.V. Ivanov, J. Crystal Growth 214/215 (2000) 130.
[17] R.T. Moug, C. Bradford, K.A. Prior, J. Crystal Growth 301–302 (2007) 289.
[18] K.A. Prior, C. Bradford, L. David, X. Tang, B.C. Cavenett, J. Crystal Growth 275 (2005) 141.